$BaRu_3Sn_6$ – A Tin-rich Stannide with $Ba@Sn_8$ and $Ru@Sn_7$ Building Units

Christian Schwickert and Rainer Pöttgen

Institut für Anorganische und Analytische Chemie, Universität Münster, Corrensstrasse 30, 48149 Münster, Germany

Reprint requests to R. Pöttgen.
E-mail: pottgen@uni-muenster.de

Z. Naturforsch. **2014**, *69b*, 481 – 485
DOI: 10.5560/ZNB.2014-4008
Received January 22, 2014

$BaRh_3Sn_6$ has been prepared by melting of the elements in a sealed tantalum tube and subsequent annealing. It crystallizes in the $BaRh_3Pb_6$-type structure: *Cmcm*, $a = 807.4(2)$, $b = 2615.3(6)$, $c = 444.0(1)$ pm, $wR = 0.0535$, 957 F^2 values, 36 variables. The structure is composed of $Ba@Sn_8$ trapezoids (349 and 353 pm Ba–Sn) and $Ru@Sn_7$ units (255–284 pm Ru–Sn) which can be derived from an octahedron by replacement of one apex by a pair of tin atoms. The $Ru@Sn_7$ units are condensed to strands *via* the trapezoidal faces, and these strands are connected to the $Ba@Sn_8$ trapezoids *via* common edges. The tin substructure of $BaRu_3Sn_6$ exhibits a broad range of Sn–Sn distances (310 – 354 pm).

Key words: Stannide, Crystal Structure, Intermetallics

Introduction

The rare earth elements form a large number of ternary stannides in combination with an electron-rich transition metal [1]. Especially the transition metals of the cobalt, nickel and copper group form many ternaries with greatly varying crystal chemistry and physical properties. When it comes to the iron group, only few stannides are known, and several structures are formed only with these transition metals. This is the case in particular for ruthenium.

So far, only few $RE_xRu_ySn_z$ stannides are known, and the reported series astonishingly exist only for the light rare earth elements: the cubic stannides $RE_3Ru_4Sn_{13}$ (RE = La, Ce, Pr, Nd) [2 – 5], $RERuSn_3$ (RE = La, Ce, Pr, Nd, Eu) [6 – 9] and related phases, the rare earth-poor phases $RERu_4Sn_6$ (RE = Y, La, Ce, Pr, Nd, Sm, Gd) [10 – 14], the ruthenium-filled $ZrSi_2$ phases $RERu_xSn_2$ (RE = La, Nd, Gd) [15, 16] as well as the equiatomic compounds CeRuSn [17] and PrRuSn [18]. Although only few of these rare earth-based phases are known, they have thoroughly been studied with respect to their properties. The $RE_3Ru_4Sn_{13}$ stannides show superconductivity [2 – 4], and heavy fermion character arises from a Kondo insulating state in $CeRu_4Sn_6$ [11, 13, 14]. $SmRuSn_3$ and $EuRuSn_3$ are interesting valence-fluctuating/mixed-valent compounds [7 – 9]. An outstanding material is CeRuSn [17, 19, 20]. It belongs to a larger family of intermetallic compounds with extremely short Ce–Ru distances which arise from the presence of almost exclusively tetravalent cerium [21, 22]. CeRuSn shows trivalent-intermediate valent cerium ordering at room temperature followed by hysteretic behavior towards low temperature, leading to a complex modulated structure.

The work on $RE_xRu_ySn_z$ stannides had been extended to include a few actinoid compounds: U_2Ru_2Sn and Np_2Ru_2Sn [23, 24] with U_3Si_2-type structure, and equiatomic URuSn [25]. An interesting result has been the high Curie temperature $T_C = 55$ K of URuSn. Many solid solutions $URu_{1-x}T_xSn$ were studied with respect to a stepwise substitution of ruthenium [26 – 30] and its consequences on the magnetic ground state.

When it comes to ternary ruthenium stannides of the alkali and alkaline earth metals, the information is scarce. Only $LiRuSn_4$ [31] and $MgRuSn_4$ [32] have been reported. $LiRuSn_4$ has been tested with respect to lithium mobility in the context of alloy electrodes on the basis of ternary tetrelides [33, 34].

In continuation of our syntheses of $SrCo_2Sn_8$ and $BaCo_2Sn_8$ [35] we started substitution experiments with other transition metals. With the heavier homolog rhodium we obtained the stannides $BaRh_{5-x}Sn_9$ and $BaRu_{5-x}Sn_9$ [36] with $BaCo_{4.7}Ge_9$ [37] structure. The phase-analytical studies in the Ba-Ru-Sn system further led to $BaRu_3Sn_6$ with $BaRh_3Pb_6$-type [38] structure. The synthesis and crystal chemistry of this new stannide are reported herein.

Experimental

Synthesis

Irregularly shaped single crystals of $BaRu_3Sn_6$ were first obtained as a by-product when exploring the homogeneity range of $BaRu_{5-x}Sn_9$. Starting materials for the targeted synthesis of $BaRu_3Sn_6$ were barium rods (Alfa Aesar, > 99 %), ruthenium powder (Sigma Aldrich, 99.9 %), and tin granules

Table 1. Crystal data and structure refinement for $BaRu_3Sn_6$.

Empirical formula	$BaRu_3Sn_6$
Formula weight, g mol^{-1}	1152.9
Unit cell dimensions (Guinier powder data)	
a, pm	807.4(2)
b, pm	2615.3(6)
c, pm	444.0(1)
V, nm^3	0.9375
Unit cell dimensions (single crystal data)	
a, pm	807.97(3)
b, pm	2615.9(1)
c, pm	443.85(1)
V, nm^3	0.9381
Space group, *Z*	*Cmcm*, 4
Calculated density, g cm^{-3}	8.17
Crystal size, μm^3	$15 \times 35 \times 50$
Transmission ratio (min/max)	0.491/0.730
Absorption coefficient, mm^{-1}	24.4
F(000), e	1952
θ range for data collection, deg	2.6 – 31.9
Range in *hkl*	± 12, ± 38, ± 6
Total no. of reflections	13 946
Independent reflections/R_{int}	957/0.0319
Reflections with $I > 3\,\sigma(I)/R_\sigma$	911/0.0062
Data/parameters	957/36
Goodness-of-fit on F^2	1.98
R/wR for $I > 3\,\sigma(I)$	0.0220/0.0528
R/wR for all data	0.0247/0.0535
Extinction coefficient	0.36(3)
Largest diff. peak/hole, e Å^{-3}	3.40/ − 2.42

(Merck, 99.9 %). Suitable barium pieces were prepared under paraffin oil, cleaned with cyclohexane (both dried over sodium wire) and kept in a Schlenk tube under argon atmosphere. The argon was purified over titanium sponge (900 K), silica gel, and molecular sieves. A polycrystalline sample was prepared by weighing the elements in stoichiometric ratio and placing them in a tantalum ampoule under an argon atmosphere of *ca*. 700 mbar. The arc-welded [39] tantalum ampoule was then sealed in an evacuated silica tube and placed in a resistance furnace. It was heated to 1300 K and kept at that temperature for 4 h. Within 72 h it was cooled to 1100 K, kept at that temperature for another 48 h and afterwards cooled to ambient temperature by radiative heat loss. The resulting ductile ingot exhibits silvery luster whereas ground powders are light grey. $BaRu_3Sn_6$ is stable in air for months.

Table 3. Interatomic distances (pm), for $BaRu_3Sn_6$ calculated with the powder lattice parameters. Standard deviations are equal to or smaller than 0.2 pm. All distances of the first coordination spheres are listed.

Ba:	4	Sn2	349.0	Sn2:	1	Ru2	272.0
	4	Sn4	352.6		2	Ru2	272.9
Ru1:	1	Sn1	262.2		1	Sn2	312.3
	2	Sn4	265.8		2	Sn2	335.4
	1	Sn3	267.7		1	Sn4	344.6
	2	Sn3	281.9		2	Ba	349.0
	1	Sn4	283.5		2	Sn1	353.6
	2	Ru1	300.0	Sn3:	2	Ru1	267.7
	1	Ru1	302.6		4	Ru1	281.9
Ru2:	1	Sn1	255.4		2	Sn4	315.7
	2	Sn2	272.0		4	Sn4	335.4
	4	Sn2	272.9	Sn4:	2	Ru1	265.8
	2	Ru2	294.7		1	Ru1	283.5
Sn1:	1	Ru2	255.4		1	Sn4	309.6
	2	Ru1	262.2		1	Sn3	315.7
	4	Sn4	349.7		2	Sn3	335.4
	4	Sn2	353.6		1	Sn2	344.6
					2	Sn1	349.7
					2	Ba	352.6

EDX data

Semiquantitative EDX analyses of the single crystal studied on the diffractometer were carried out in variable pressure mode with a Zeiss EVO® MA10 scanning electron microscope with BaF_2, Ru and Sn as standards. The experimentally observed average composition (10 ± 1 at.-% Ba : 30 ± 1 at.-% Ru : 60 ± 1 at.-% Sn) was close to the ideal one. No impurity elements heavier than sodium (detection limit of the instrument) were detected.

X-Ray diffraction

The polycrystalline $BaRu_3Sn_6$ sample was studied by powder X-ray diffraction using the Guinier technique: imag-

Table 2. Atomic coordinates and anisotropic displacement parameters (pm^2) for $BaRu_3Sn_6$. U_{eq} is defined as one third of the trace of the orthogonalized U_{ij} tensor.

Atom	Site	*x*	*y*	*z*	U_{11}	U_{22}	U_{33}	U_{12}	U_{eq}
Ba	4*c*	0	0.58858(2)	1/4	126(2)	184(2)	79(2)	0	130(1)
Ru1	8*g*	0.18741(5)	0.21661(2)	1/4	65(2)	71(2)	54(2)	−9(1)	63(1)
Ru2	4*c*	0	0.03706(2)	1/4	121(3)	47(2)	45(2)	0	71(1)
Sn1	4*c*	0	0.13471(2)	1/4	113(2)	48(2)	125(3)	0	95(1)
Sn2	8*g*	0.80659(5)	0.95193(2)	1/4	132(2)	156(2)	79(2)	−64(1)	122(1)
Sn3	4*c*	0	0.75072(2)	1/4	51(2)	102(2)	69(2)	0	74(1)
Sn4	8*g*	0.19175(5)	0.32501(1)	1/4	97(2)	93(2)	65(2)	22(1)	85(1)

ing plate detector (Fujifilm BAS-1800), CuK_{α_1} radiation and α-quartz ($a = 491.30$, $c = 540.46$ pm) as an internal standard. The orthorhombic lattice parameters (Table 1) were refined on the basis of the Guinier data by a standard least-squares refinement. Correct indexing of the pattern was ensured through an intensity calculation [40]. The single crystal and powder lattice parameters agreed well.

Irregularly-shaped single crystals of $BaRu_3Sn_6$ were selected from the crushed annealed sample. The crystals were glued to quartz fibers using beeswax, and their quality was checked on a Buerger camera (using white Mo radiation). Intensity data of a suitable crystal were collected on a Stoe IPDS-II image plate system (graphite-monochromatized Mo radiation; $\lambda = 71.073$ pm) in oscillation mode. A numerical absorption correction was applied to the data set. Details about the data collection and the crystallographic parameters are listed in Table 1.

Structure determination and refinement

Analyses of the $BaRu_3Sn_6$ data set revealed a *C*-centered orthorhombic lattice, and the systematic extinction conditions were in agreement with the space groups $Cmc2_1$ and *Cmcm*, of which the centrosymmetric group was found correct during structure refinement. The starting atomic parameters were deduced using the charge-flipping algorithm of SUPERFLIP [41], and the structure was refined with anisotropic displacement parameters for all atoms with JANA2006 [42]. The solution of the structure revealed the Pearson code *oS*40 with Wyckoff sequence g^3c^4. Inspection of the Pearson data base [43] readily indicated isotypism with $BaRh_3Pb_6$ [38].

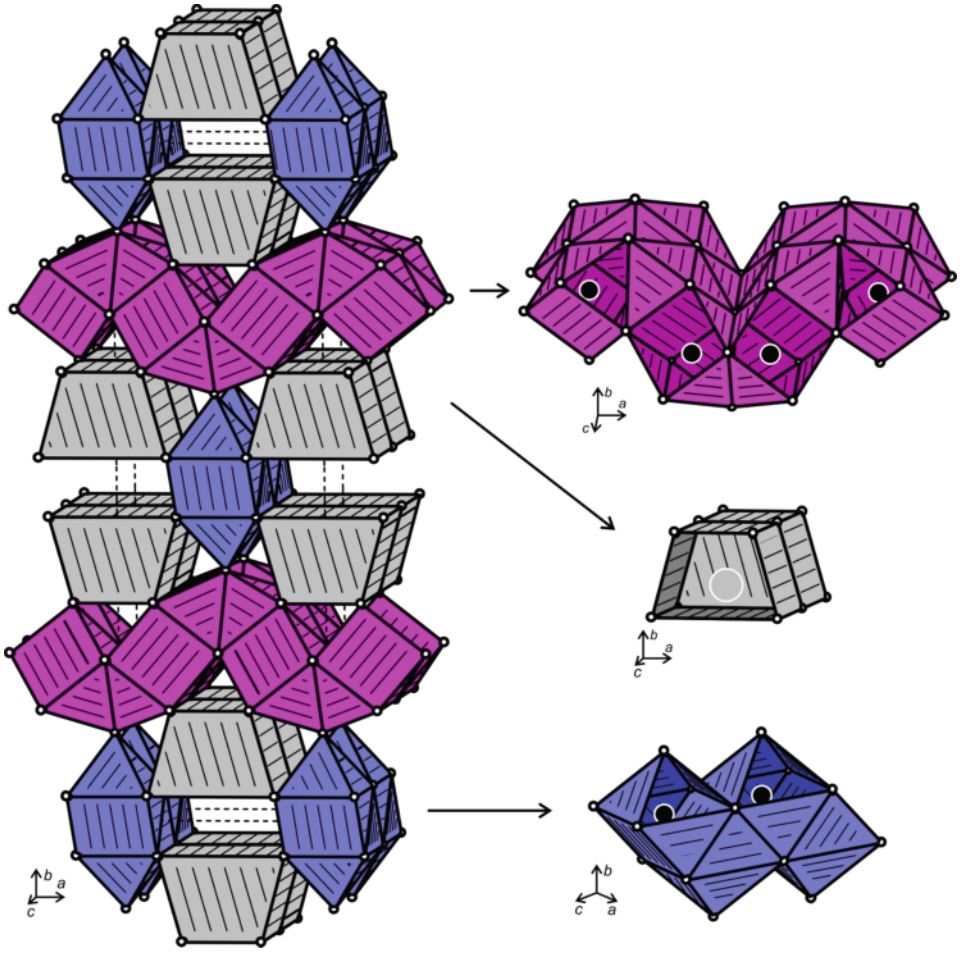

Fig. 1 (color online). The crystal structure of $BaRu_3Sn_6$. The unit cell is presented at the left side. The condensation pattern of the Ba@Sn_8 (light grey), Ru1@Sn_7 (magenta) and Ru2@Sn_7 (blue) polyhedra is emphasized with partially open polyhedra at the right side.

The $BaRu_3Sn_6$ structure was then refined with the setting of the prototype. Separate refinements of the occupancy parameters gave no hint for deviations from the ideal composition. All sites were fully occupied within two standard deviations. The final difference Fourier syntheses revealed no residual peaks. The refined atomic positions, displacement parameters, and interatomic distances are given in Tables 2 and 3.

Further details of the crystal structure investigation may be obtained from Fachinformationszentrum Karlsruhe, 76344 Eggenstein-Leopoldshafen, Germany (fax: +49-7247-808-666; e-mail: crysdata@fiz-karlsruhe.de, http://www.fiz-karlsruhe.de/request_for_deposited_data.html) on quoting the deposition number CSD-427286.

Discussion

Crystal chemistry

The tin-rich stannide $BaRu_3Sn_6$ crystallizes with the $BaRh_3Pb_6$-type [38] structure, space group *Cmcm*, Pearson code *oS*40, Wyckoff sequence g^3c^4. It is one of the few ternary stannides of the alkali and alkaline earth metals with electron-rich transition metals [43, 44].

The $BaRu_3Sn_6$ structure has seven crystallographically independent sites, Ba, Ru1, Ru2, and four tin sites. The unit cell is not that large, but the structure seems complex at first sight. A simple description is possible through the polyhedra around the barium and ruthenium atoms (Fig. 1). Each barium atom has eight nearest tin neighbors at Ba–Sn distances of 349 – 353 pm. These tin neighbors are arranged in form of a trapezoid, and they are condensed along the *c* axis *via* common trapezoidal faces. This is a comparatively low coordination number for the barium atoms, keeping in mind that the Ru1 atoms as next nearest neighbors are already at Ba–Ru1 distances of 419 pm. Similar barium coordinations occur in $BaCu_9Sn_4$ with $Ba@Sn_8$ (356 pm) [45], Ba_3Sn_5 with $Ba1@Sn_9$ (349 – 388 pm) and $Ba2@Sn_{10}$ (357 – 381 pm) [46].

Both ruthenium sites have coordination number 7 with Ru–Sn distances covering the broad range from 255 to 284 pm, close to the sum of the covalent radii of 265 pm [47]. Smaller coordination numbers occur in TiNiSi-type PrRuSn ($RuSn_{4/4}$ tetrahedra with 268 – 274 pm) [18] and $CeRu_4Sn_6$ ($RuSn_{6/4}$ octahedra with 257 – 277 pm) [11]. The so far largest coordination number has been observed for $MgRuSn_4$ [32]: $Ru@Sn_8$ antiprisms with 284 pm Ru–Sn.

The $Ru@Sn_7$ units in $BaRu_3Sn_6$ can be derived from a centered octahedron of which one apex is substituted by a pair of tin atoms. Different modes of condensation of the $Ru@Sn_7$ units lead two separate substructures. The $Ru2@Sn_7$ units condense *via* the two rectangular faces, and these infinite strands extend along *c* (Fig. 1, blue substructure). Such strands are also formed for the $Ru1@Sn_7$ units (Fig. 1, magenta substructure), however, adjacent strands are further condensed *via* common triangles, leading to the two-dimensional substructure. The three polyhedral building units are then condensed *via* common corners and edges. Similar to the highly condensed octahedra in $CeRu_4Sn_6$ [11], we also observe closer Ru–Ru contacts (295 – 303 pm) between the centers of the $Ru@Sn_7$ units. These Ru–Ru distances are all longer than in *hcp* ruthenium (6×265 and 6×271 pm) [48], and we can assume only weak Ru–Ru bonding in $BaRu_3Sn_6$.

As expected from the high tin content, one observes a broad range of Sn–Sn distances (310 – 354 pm). The shorter Sn–Sn distances fit with those in the β-Sn structure (4×302 and 2×318 pm) [48]. The longer ones can be considered as secondary, weak Sn–Sn interactions. This bonding situation is similar to that in $BaCo_2Sn_8$ [35].

Acknowledgement

We thank Dipl.-Ing. U. Ch. Rodewald for the intensity data collection. This work was supported by the Deutsche Forschungsgemeinschaft.

[1] R. V. Skolozdra in *Handbook on the Physics and Chemistry of Rare Earths*, (Eds.: K. A. Gschneidner, Jr., L. Eyring), Elsevier Science, Amsterdam, **1997**, chapter 164, pp. 399 – 517.
[2] A. S. Cooper, *Mater. Res. Bull.* **1980**, *15*, 799.
[3] G. P. Espinosa, A. S. Cooper, H. Barz, J. P. Remeika, *Mater. Res. Bull.* **1980**, *15*, 1635.
[4] G. P. Espinosa, A. S. Cooper, H. Barz, *Mater. Res. Bull.* **1982**, *17*, 963.
[5] T. Mishra, C. Schwickert, T. Langer, R. Pöttgen, *Z. Naturforsch.* **2011**, *66b*, 664.
[6] B. Eisenmann, H. Schäfer, *J. Less-Common Met.* **1986**, *123*, 89.
[7] T. Fukuhara, S. Iwakawa, H. Sato, *J. Magn. Magn. Mater.* **1992**, *104 – 107*, 667.
[8] C. Godart, C. Mazumdar, S. K. Dhar, R. Nagarajan, L. C. Gupta, B. D. Padalia, R. Vijayaraghavan, *Phys. Rev. B* **1993**, *48*, 16402.
[9] T. Harmening, W. Hermes, M. Eul, R. Pöttgen, *Solid State Sci.* **2010**, *12*, 284.
[10] G. Venturini, B. Chafik El Idrissi, J. F. Marêché, B. Malaman, *Mater. Res. Bull.* **1990**, *25*, 1541.

[11] R. Pöttgen, R.-D. Hoffmann, E. V. Sampathkumaran, I. Das, B. D. Mosel, R. Müllmann, *J. Solid State Chem.* **1997**, *134*, 326.

[12] M. F. Zumdick, R. Pöttgen, *Z. Naturforsch.* **1999**, *54b*, 863.

[13] E. M. Brüning, M. Brando, M. Baenitz, A. Bentien, A. M. Strydom, R. E. Walstedt, F. Steglich, *Phys. Rev. B* **2010**, *82*, 125115.

[14] V. Guritanu, P. Wissgott, T. Weig, H. Winkler, J. Sichelschmidt, M. Scheffler, A. Prokofiev, S. Kimura, T. Iizuka, A. M. Strydom, M. Dressel, F. Steglich, K. Held, S. Paschen, *Phys. Rev. B* **2013**, *87*, 115129.

[15] M. François, G. Venturini, B. Malaman, B. Roques, *J. Less-Common Met.* **1990**, *160*, 197.

[16] P. Salamakha, P. Demchenko, J. Stępień-Damm, *J. Alloys Compd.* **1997**, *260*, L1.

[17] J. F. Riecken, W. Hermes, B. Chevalier, R.-D. Hoffmann, F. M. Schappacher, R. Pöttgen, *Z. Anorg. Allg. Chem.* **2007**, *633*, 1094.

[18] J. F. Riecken, A. F. Al Alam, B. Chevalier, S. F. Matar, R. Pöttgen, *Z. Naturforsch.* **2008**, *63b*, 1062.

[19] S. F. Matar, J. F. Riecken, B. Chevalier, R. Pöttgen, V. Eyert, *Phys. Rev. B* **2007**, *76*, 174434.

[20] J. Mydosh, A. M. Strydom, M. Baenitz, B. Chevalier, W. Hermes, R. Pöttgen, *Phys. Rev. B* **2011**, *83*, 054411.

[21] W. Hermes, S. F. Matar, R. Pöttgen, *Z. Naturforsch.* **2009**, *64b*, 901.

[22] T. Mishra, R.-D. Hoffmann, C. Schwickert, R. Pöttgen, *Z. Naturforsch.* **2011**, *66b*, 771.

[23] L. C. J. Pereira, J. M. Winand, F. Wastin, J. Rebizant, J. C. Spirlet, *24^{ièmes} Journées des Actinides*, Abstract PB9, Obergurgl (Austria) **1994**, pp. 109.

[24] F. Mirambet, B. Chevalier, L. Fournès, P. Gravereau, J. Etourneau, *J. Alloys Compd.* **1994**, *203*, 29.

[25] A. V. Andreev, M. I. Bartashevich, *Fiz. Met. Metalloved.* **1986**, *62*, 266.

[26] V. Sechovský, L. Havela, L. Neužil, A. V. Andreev, G. Hilscher, C. Schmitzer, *J. Less-Common Met.* **1986**, *121*, 169.

[27] T. T. M. Palstra, G. J. Nieuwenhuys, R. F. M. Vlastuin, J. van den Berg, J. A. Mydosh, K. H. J. Buschow, *J. Magn. Magn. Mater.* **1987**, *67*, 331.

[28] A. V. Andreev, H. Aruga Katori, T. Goto, V. Sechovský, L. Havela, *J. Magn. Magn. Mater.* **1995**, *140–144*, 1383.

[29] T. D. Cuong, Z. Arnold, J. Kamarád, A. V. Andreev, L. Havela, V. Sechovský, *J. Magn. Magn. Mater.* **1996**, *157/158*, 694.

[30] L. Havela, K. Miliyanchuk, A. V. Kolomiets, L. C. J. Pereira, A. P. Gonçalves, E. Šantavá, K. Prokeš, *J. Alloys Compd.* **2007**, *446–447*, 606.

[31] Z. Wu, R.-D. Hoffmann, R. Pöttgen, *Z. Anorg. Allg. Chem.* **2002**, *628*, 1484.

[32] M. Schlüter, A. Kunst, R. Pöttgen, *Z. Anorg. Allg. Chem.* **2002**, *628*, 2641.

[33] Zh. Wu, H. Eckert, J. Senker, D. Johrendt, G. Kotzyba, B. D. Mosel, H. Trill, R.-D. Hoffmann, R. Pöttgen, *J. Phys. Chem. B* **2003**, *107*, 1943.

[34] R. Pöttgen, T. Dinges, H. Eckert, P. Sreeraj, H.-D. Wiemhöfer, *Z. Phys. Chem.* **2010**, *224*, 1475.

[35] C. Schwickert, R. Pöttgen, *Z. Naturforsch.* **2013**, *68b*, 17.

[36] C. Schwickert, R. Pöttgen, *Monatsh. Chem.* **2014**, submitted for publication.

[37] N. Nasir, N. Melnychenko-Koblyuk, A. Grytsiv, P. Rogl, E. Bauer, E. Royanian, H. Michor, G. Hilscher, G. Giester, *Intermetallics* **2009**, *17*, 471.

[38] G. Venturini, M. Kamta, B. Malaman, J. F. Marêché, B. Roques, *Mater. Res. Bull.* **1987**, *22*, 359.

[39] R. Pöttgen, Th. Gulden, A. Simon, *GIT Labor-Fachzeitschrift* **1999**, *43*, 133.

[40] K. Yvon, W. Jeitschko, E. Parthé, *J. Appl. Crystallogr.* **1977**, *10*, 73.

[41] L. Palatinus, G. Chapuis, *J. Appl. Crystallogr.* **2007**, *40*, 786.

[42] V. Petricek, M. Dusek, L. Palatinus, JANA2006, The Crystallographic Computing System, Institute of Physics, University of Prague, Prague (Czech Republic) **2006**.

[43] P. Villars, K. Cenzual, *Pearson's Crystal Data - Crystal Structure Database for Inorganic Compounds* (release 2013/14), ASM International, Materials Park, Ohio (USA) **2013**.

[44] R. Pöttgen, *Z. Naturforsch.* **2006**, *61b*, 677.

[45] M. Pani, M. L. Fornasini, P. Manfrinetti, F. Merlo, *Intermetallics* **2011**, *19*, 957.

[46] F. Zürcher, R. Nesper, S. Hoffmann, T. F. Fässler, *Z. Anorg. Allg. Chem.* **2001**, *627*, 2211.

[47] J. Emsley, *The Elements*, Oxford University Press, Oxford **1999**.

[48] J. Donohue, *The Structures of the Elements*, Wiley, New York **1974**.